

Finite Element Analysis Of Drum Brake Assembly

Na Liu^a, Zhongcai Zheng^{*a}, Yalan Wu^a, Xiangan Kong^a, Hang Ding^b

^aSchool of Mechanical and Electrical Engineering, Shandong Jianzhu University, Jinan, 250101, China,

^bSchool of Mechanical Engineering, Jinan University, Jinan, 250022, China.

zzc638@163.com

Finite element analysis of automobile drum brake assembly was made in this article. First brake drum assembly 3D model including brake drum, brake shoe, brake block, and friction plate was established; then finite element analysis of drum brake assembly was made, considering the friction between assemblies as well as the relative sliding between brake shoe and brake block, brake block and friction plate. The simulation of automobile's braking was relatively authentic, drum brake's stress and displacement deformation at work was analyzed. The results showed that with fixed brake drum, left and right brake shoes' load was completely symmetric, stress and displacement distribution was also completely symmetric; in the process of braking, one side brake shoe's stress and displacement were obviously bigger than the other side, max stress occurred on one side brake shoe's internal end face.

1. Introduction

Brake is the most important safety components in automobile braking system (Chen Jiarui (2010), Fang Yonglong (2005), Benincá (2015), Yu Zhisheng (2009), Abd Rahman (2014)), and it has great meaning to make in-depth analysis of automobile brake (Abu-Bakar (2009), John Fenton (1996), Lee, J.M (2001), Pereira (2013), Hamid (2013)). This article made a certain car's drum brake research object and made calculation and analysis with finite element analysis software.

2. Buildup of Model

2.1 Buildup of Parts Model

Before model drawing, this model's specific structure and size should be made clear. It was suggested that this modeling adapt the car drum brake's size and structure and make simplification to it. Schematic structure of drum brake was as shown in figure 1. The simplified drum brake assemble (Rudolf (1992), Shi Wenku (2005),) was made up of 7 parts: brake drum, left and right brake shoes, two pieces of brake blocks and two pieces of friction plates, in which left and right brake shoes, two pieces of brake blocks and two pieces of friction plates were completely symmetry. Left shoe assemble can be made first, then right shoe assemble was generated using Mirror when assembling. Figure 2(a-d) are respectively 3D model of brake drum, brake shoe, brake block and friction plate already built.

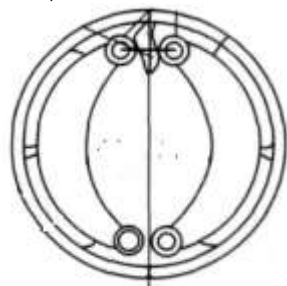


Figure 1: Schematic structure of drum brake



(a) 3D model of brake drum (b) 3D model of brake shoe (c) 3D model of brake block (d) 3D model of friction plate

Figure 2: 3D model of brake component

2.2 Assembly of Brake Parts

Well-built part models were fitted and brake assembly was generated. As brake working conditions simulation was needed to make finite analysis, brake shoes assembly should rotate around the pin to be tangent to brake drum. This assembly constrain was a difficulty. Brake shoe and brake block, as well as brake block and friction plate were mutually restrained by contact. Then rotate restrained brake shoe assembly around the pin to be tangent to brake drum. Figure 3 is brake assembly built well.

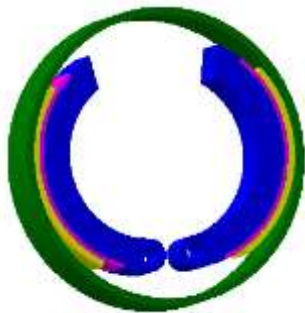


Figure 3: Assembly of brake module

3. Build-up of Brake Assembly' Finite Element Model

3.1 Grid Generation

Firstly grid generation to well-built brake assembly was made. First order tetrahedral grid C3D4 was adopted. Sum total of grids was 157516 as divided. Generated unit sums are shown in Table one. Generated grid model figure are shown in Figure 4. In the process of grid generation, in addition to paying attention to grids quantity, grid generation on mutual contacting components' contacting surface should be well coordinated. Namely grids' shape and size should be as consistent as possible, so as to get fair convergence in finite element calculating and analyzing.

Table 1: Brake module's grid cell attribute

Name of parts	Unit type	No. of units
Brake drum	First order tetrahedral C3D4	62094
Left brake shoe	First order tetrahedral C3D4	31755
Left brake block	First order tetrahedral C3D4	6535
Left friction plate	First order tetrahedral C3D4	9445
Right brake shoe	First order tetrahedral C3D4	31699
Right brake block	First order tetrahedral C3D4	6497
Right friction plate	First order tetrahedral C3D4	9491



Figure 4: Brake assembly grid model

In order to correctly define contact relation in finite element analysis, module parts' contact surfaces needed to be defined as well. 6 pairs of 12 contact surfaces were needed to set up this assembly structure. There were 2 pairs of contact surface between brake drum and left/right friction plates, 2 pairs of contact surface between left/right friction plates and left/right brake plates, and 2 pairs of contact surface between left/right brake plates and left/right brake shoes. In addition, impel power applying loading surface would be built up.

3.2 Definition of Material Property

On the basis of material applied in and consulting relevant material manual, components' material property was obtained and showed in Table 2.

Table 2: Brake module components' material property

Name of parts	Material	Density/kg·m ⁻³	Young Modulus /MPa	Poisson's Ratio	Strength of Extension
Brake drum	HT250	7200	130000	0.25	0.25
Left brake shoe	HT200	7200	80000	0.25	0.25
Left brake block	HT200	7200	80000	0.25	0.25
Left friction plate	moulded material	2000	13000	0.4	0.4
Right brake shoe	HT200	7200	80000	0.25	0.25
Right brake block	HT200	7200	80000	0.25	0.25
Right friction plate	moulded material	2000	13000	0.4	0.4

3.3 Build-up of Contacting Relation

Contacting relations of the 7 pairs of contact surfaces established in Section 3.1 was defined, in which tie binding constraints was adopted between friction plate and brake block, as well as between brake block and brake shoes. General frictional contact was adopted between friction plate and brake drum. Selection of friction films, not only hope that the friction coefficient is higher, and the fever is good, the temperature and pressure effect. High friction coefficient is not easy for the pursuit of friction materials. We should increase the stability of the friction coefficient and reduce the sensitivity of the brake to the deviation of the normal value of the friction coefficient. In general, the higher the friction coefficient, the worse the wear resistance of the material. Therefore, under the assumption of ideal conditions to calculate the brake torque, the $f=0.3$ can make the calculation results close to the actual value.

3.4 Load and Boundary Conditions

Reasonable load and right constrain applied on finite element model were directly related to the accuracy of finite element calculation results. This model's only external applied load was wheel cylinder impel power's effect, whose strength and function direction given by foregoing chapters. In order to simulate the relative sliding between brake drum and friction plate, as well as exert rotational displacement to drum and solve the braking torque more easily, coupling rigid connection unit was applied on drum's end face, and center node was drum's axis. Displacement boundary condition was relatively complicated: for brake shoe, pin hole internal end face degrees freedom was constrained, only rotation degrees freedom around the axis was reserved; for brake drum, brake drum coupling center node degrees freedom was constrained, only rotation degrees freedom around the axis was reserved.

Drum brake force diagram was as shown in Figure 5. According to the calculation of certain parameters, impel power was exerted on contact surface between brake shoe and brake cylinder, with power of 7050N. When making finite element calculation, this load was exerted by uniform pressure load. To change impel power load into pressure load, it only need to be divided by brake area. Brake area can be acquired by measuring three-dimensional geometrical modeling's corresponding surface, which is 1374.256 mm², and magnitude of load was acquired as 5.13MPa.

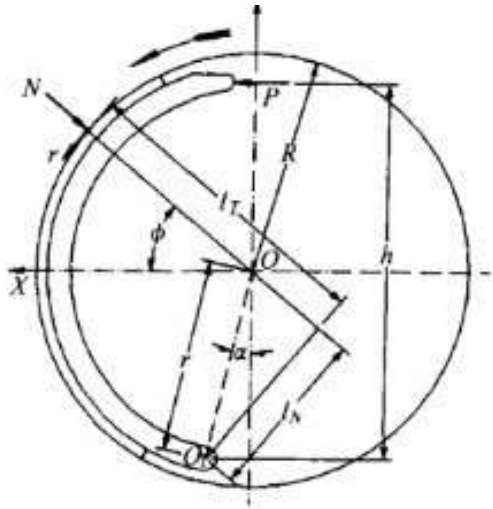


Figure 5: Drum brake force diagram

4. Calculation and Solution

Finite element solver was used to solve. In order to simulate the contact relation between brake shoe module and brake drum, it was accomplished by two steps. First fix the brake drum, and brake shoe components would press brake drum tight under the effect of impel power. This process had no brake torque, so left and right shoes' results should be symmetric. Then rotate brake drum coupling center node displacement for a small angle, and rely micro dependent variable to simulate the generating of brake torque.

5. Result Analysis

5.1 Results of Fixed Brake Drum

Brake drum had no displacement in this process. As left and right brake shoes' load was completely symmetric, the distribution of stress and displacement was also completely symmetric. Figure 6 and 7 are brake shoe module' stress nephogram and displacement nephogram. As there were no brake torque applied, stress value was smaller, max stress only 5.638MPa, almost equal with impel power load.

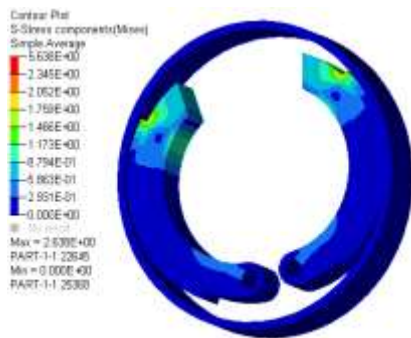


Figure 6: Brake shoe module stress nephogram

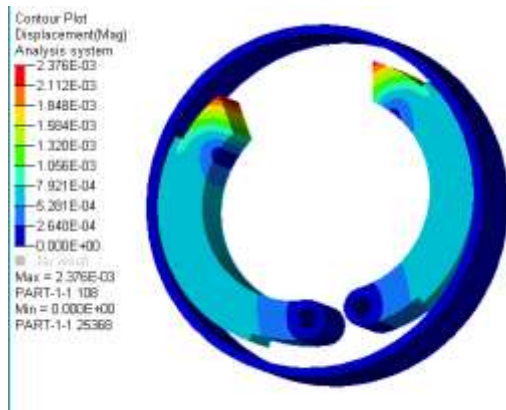


Figure 7: Brake shoe module displacement nephogram

5.2 Results of Brake Drum with Displacement and Strain

In this process, as small rotational displacement was applied to brake drum to simulate brake torque, left and right brake shoes' stress and displacement became not symmetric any more. This process needed to apply displacement to brake drum, so unlike 5.1's analysis, it calculated and output brake drum's calculation. Figure 8 and 9 are brake module's stress nephogram and displacement nephogram.

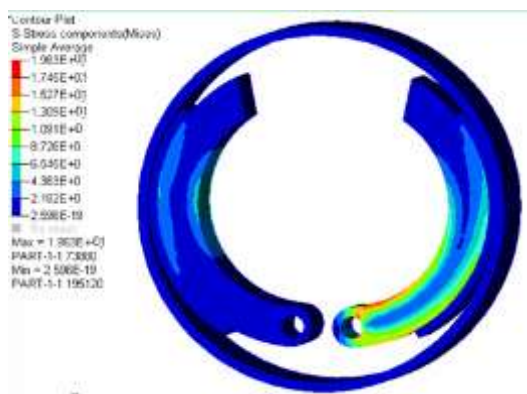


Figure 8: Brake module's stress nephogram

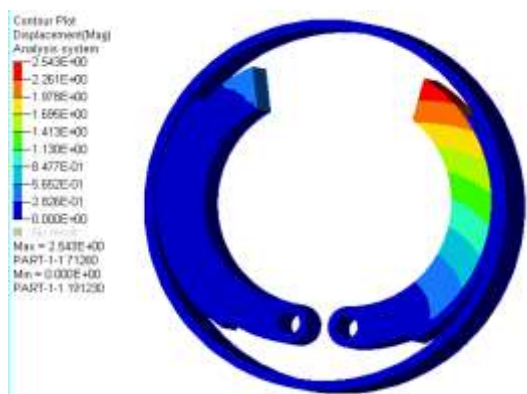


Figure 9: Brake module's displacement nephogram

As can be seen from the figure, one side brake shoe's stress and displacement were obviously bigger than the other side, which was completely in conformity with leading trailing shoe brake's operating principle that is one side's braking force was greater than the other side's (Nguyen (2015), Kaminsk (2013), Van (2012)). This result had reasonability. As is shown in stress nephogram, max stress occurred on one side brake shoe's

internal end face. Max stress value was 19.63MPa, which was far less than material's compression strength value. Therefore this design's drum brake module's strength can meet requirements.

6. Conclusions

By infinite element analysis of brakes, the following conclusion can be drawn:

(1) With fixed brake drum, left and right brake shoes' load was completely symmetric, so stress and displacement distribution was also completely symmetric. Figure 4 and 5 are brake drum module's stress nephogram and displacement nephogram. As there was no brake torque applied, stress value was smaller, max stress only 5.638MPa, almost equal with impel power load.

(2) In the process of braking, one side brake shoe's stress and displacement were obviously bigger than the other side, which was completely in conformity with leading trailing shoe brake's operating principle, that is one side's braking force was greater than the other side's. This result has reasonability. As is shown in stress nephogram, max stress occurred on one side brake shoe's internal end face. Max stress value was 19.63MPa, which was far less than material's compression strength value. Therefore this design's drum brake assembly's strength met requirements.

References

- Abd Rahman M.R., Vernin G., Bakar A.R.A., 2014, Preventing drum brake squeal through lining modifications, *Applied Mechanics and Materials*, 471, 20-24, DOI: 10.4028/www.scientific.net/AMM.471.20
- Abd Rahim A.B. etc, 2009, Suppression of drum brake squeal through structural modifications using finite element method, *International Journal of Vehicle Design*, 51(1-2), 3-20
- Benincá E. etc, 2015, Thermal Influence on Friction Material Wearing for City Buses Application, *SAE Technical Papers*, 2015-May(1), DOI: 10.4271/2015-36-0009
- Chen J.R., 2010, *Automobile Structure*, Beijing: People's Communications Press
- Fang Y.L., 2005 *Automobile Brake Theory And Design*, Beijing: national defense industry press,
- Hamid M.N.A., Ripin Z.M., 2013, Effect of drum radius variation on the brake torque variation and brake factor, *International Journal of Vehicle Design*, 63(4), 404-422, DOI: 10.1504/IJVD.2013.057473
- John F., 1996, *Hand Book of Vehicle Design Analysis*. Warrendale, PA. USA: Society of Automotice Engineers, Inc.
- Kaminski, Z., 2013, Experimental and numerical studies of mechanical subsystem for simulation of agricultural trailer air braking systems, *International Journal of Heavy Vehicle Systems*, 20(4), 289-311, DOI: 10.1504/IJHVS.2013.056802
- Lee, J.M., 2001, A study on the squeal of a drum brake which has shoes of non-uniform cross-section, *Journal of Sound and Vibration*, 240(5), 789-808
- Limpert R., 1992, *BRAKE DESSIGN and ASFETY*. Warrendale, PA 15096, USA: SAE, Inc
- Nguyen Q.H., Lang V.T., Choi S.B., 2015, Optimal design and selection of magneto-rheological brake types based on braking torque and mass, *Smart Materials and Structures*, 24(6), DOI: 10.1088/0964-1726/24/6/067001
- Pereira, M.H. etc, 2013, Designing a lightweight drum brake component using fem and metal forming competences, 22nd SAE Brasil International Congress and Display, *SAE Technical Papers*, 13, BRASILCONG 2013, DOI: 10.4271/2013-36-0617
- Shi W.K., 2005, *Modern Automotive Technology*, Beijing: National Defense Industry Press.
- Wittenberghe J.V., Ost W., Baets P.D., 2012, Testing the friction characteristics of industrial drum brake linings, *Experimental Techniques*, 36(1), 43-49, DOI: 10.1111/j.1747-1567.2010.00675.x
- Yu Z.S., 2009, *Automotive Theory*, Beijing: machinery industry press